

Kinetics and Mechanism of the Tropospheric Reaction of 3-Hydroxy-3-methyl-2-butanone with Cl Atoms

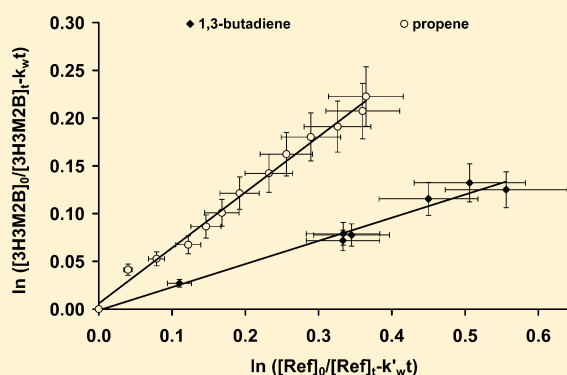
C. Sleiman,[†] G. El Dib,^{*,†} B. Ballesteros,[‡] A. Moreno,[‡] J. Albaladejo,[‡] A. Canosa,[†] and A. Chakir[§]

[†]Département de Physique Moléculaire, Institut de Physique de Rennes, UMR 6251 du CNRS - Université de Rennes 1, Bat. 11C, Campus de Beaulieu, 35042 Rennes Cedex, France

[‡]Facultad de Ciencias y Tecnologías Químicas, Departamento de Química Física, Universidad de Castilla La Mancha, Campus Universitario, 13071 Ciudad Real, Spain

[§]Laboratoire GSMA-UMR 6089 CNRS, Université de Reims, Campus Moulin de la Housse, BP 1039, 51687 Reims Cedex 02, France

ABSTRACT: The relative rate coefficient for the gas-phase reaction of 3-hydroxy-3-methyl-2-butanone (3H3M2B) with Cl atoms was determined under atmospheric conditions (298 ± 2 K, 720 ± 2 Torr). The products of the reaction were identified and quantified. This work provides the first kinetic and mechanistic determinations of the gas-phase reaction of Cl atoms with 3H3M2B. The rate measurements and the products studies were performed in two simulation chambers coupled to the gas chromatography–mass spectrometer (GC–MS) and the Fourier transform infrared (FTIR) techniques, respectively. The obtained average rate coefficient was $(1.13 \pm 0.17) \times 10^{-10}$ cm³ molecule⁻¹ s⁻¹ using propene and 1,3-butadiene as reference compounds. The major primary reaction products observed in this study were (with % molar yields): acetic acid (42.6 ± 4.8) and 2,3-butanedione (17.2 ± 2.3). Results and mechanism are discussed in terms of the structure–reactivity relationship and compared with the reported reactivity with the other atmospheric oxidants. The atmospheric implications derived from this study are discussed as well.



1. INTRODUCTION

Carbonyl compounds play an important role in atmospheric chemistry and in urban air pollution. In fact, these species widely contribute to the formation of free radicals that are responsible for the oxidation of hydrocarbons.¹ They are also precursors of other oxidants such as ozone, peroxyacyl nitrates (PANs), and nitric acid and are important intermediates in aerosol formation.² Carbonyl compounds are directly emitted into the troposphere from biogenic and anthropogenic sources^{3–5} and are also major reaction products in the atmospheric oxidation of unsaturated hydrocarbons and other volatile organic compounds (VOCs).⁶

Among the carbonyl compounds released into the atmosphere, hydroxycarbonyls are a variety of multifunctional organic molecules that are formed from the atmospheric degradation of anthropogenically or naturally emitted VOCs. Furthermore, hydroxycarbonyls are used in a number of industrial sectors namely in food,⁷ chemicals, and pharmaceutical synthesis.⁸

Hydroxyketones constitute a large category of hydroxycarbonyls. Despite the importance of these species in atmospheric chemistry, so far most of the performed studies concerning the reactivity of these compounds have been focused on hydroxyacetone HOCH₂C(O)CH₃, which is formed during the atmospheric oxidation of isoprene, the most important biogenically emitted non-methane hydrocarbon.⁹ Kinetic and

mechanistic studies of the reaction of hydroxyacetone with OH and Cl have been carried out at different temperatures.^{9–13} However, very little information exists concerning the atmospheric fate of longer chain C₄-hydroxyketones. In fact, only four kinetic studies on the gas-phase reaction of C₄-hydroxyketones can be found in the literature. Three of these studies have been carried out at atmospheric pressure using a relative technique. Aschmann et al.¹⁴ studied the reaction of a series of hydroxyketones including four C₄-hydroxyketones, with OH, NO₃, and O₃. The obtained results indicated that the degradation of these hydroxyketones was dominated by their gas-phase reaction with the OH radical. In the study carried out by Baker et al.¹⁵ two C₄-hydroxyketones (1-hydroxy-2-butanone and 4-hydroxy-2-butanone) were identified as products of the reactions of butanediols with OH. The kinetics of these hydroxyketones with OH was measured as well. Very recently, Messaadia et al.¹⁶ investigated the gas-phase reactions of 3-hydroxy-2-butanone and 4-hydroxy-2-butanone with OH radicals as a function of temperature and the reaction with Cl atoms at room temperature using a relative rate method. A slight negative dependence of the rate coefficients behavior was observed for reactions with OH. Moreover, an absolute rate

Received: June 2, 2014

Revised: July 25, 2014

Published: July 28, 2014

coefficient for the reaction of 4-hydroxy-2-butanone with OH was measured by El Dib et al.,¹⁷ by vapor pressure measurements of 4-hydroxy-2-butanone. This study was carried out at room temperature and over the pressure range 10–330 Torr in He and synthetic air as diluents gases. In addition, the removal of these species due to photolysis has been studied by Messaadia et al.¹⁸ and upper limits of the UV photolysis rates of a series of C₄-hydroxyketones have been estimated by the authors. The obtained values showed that photolysis could be an important loss process of these species in the Earth atmosphere.

The present work reports the first kinetic and mechanistic studies of the gas-phase reaction of Cl atoms with 3-hydroxy-3-methyl-2-butanone 3H3M2B, ((CH₃)₂C(OH)C(O)CH₃), a C₄ carbon chain hydroxyketone where the OH group is in the α position with respect to the carbonyl group.

In the atmosphere, like other carbonyl compounds, 3H3M2B is expected to be removed by chemical reactions with the atmospheric photooxidants and by photolysis. The atmospheric degradation of 3H3M2B is, however, not well-known. In fact, only one kinetic study on the gas-phase reaction of 3H3M2B is found in the literature.¹⁴ In this study, the degradation of 3H3M2B due to its reaction with OH, NO₃, and O₃ has been investigated at room temperature and atmospheric pressure using a relative technique. A rate coefficient of $(0.94 \pm 0.37) \times 10^{-12}$ cm³ molecule⁻¹ s⁻¹ was obtained for the reaction of 3H3M2B with OH. Upper limits of 2×10^{-16} cm³ molecule⁻¹ s⁻¹ and 1.1×10^{-19} cm³ molecule⁻¹ s⁻¹ were obtained for reactions with NO₃ radicals and O₃, respectively. In addition, the tropospheric lifetime of 3H3M2B due to photolysis has been estimated by Messaadia et al.¹⁸ to be at least 0.4 day using an upper limit of the photolysis rate assuming a quantum yield of unity.

Despite the significant role of Cl atoms in the atmospheric chemistry, there are no data reported in the literature on the atmospheric oxidation of 3H3M2B with Cl atoms. In fact, the chemistry of Cl atoms plays an important role in the oxidizing capacity of the troposphere particularly in the early morning in continental regions, in coastal and marine air environments and in the Arctic troposphere during springtime.^{19–24} Although the peak of Cl atom concentrations (10^5 atoms cm⁻³)²⁵ is much lower than that of OH radicals (10^6 atoms cm⁻³),^{26,27} the two reactions can compete with one another in areas where the chlorine atom concentration is sufficiently high since rate coefficients for the reactions of Cl atoms with organic compounds are generally a factor of 10 higher than the corresponding OH rate coefficients.²⁸ The aim of the present study is to assess the importance of the reaction of Cl atoms as an atmospheric loss process of 3H3M2B. The results are used to calculate the effective lifetime of 3H3M2B in the troposphere and to better define the reactivity of the studied compound toward the Cl atoms and for a better understanding of its atmospheric fate.

2. EXPERIMENTAL SECTION

2.1. Relative Rate Coefficient Measurements. The relative Cl-kinetic measurements were carried out in two environmental chambers equipped with FTIR and GC–MS in the presence of reference compounds as explained below. A detailed description of the experimental setup and the kinetic analysis performed has been previously presented.^{29–31} Thus, the experimental system will be only briefly described here.

The first environmental chamber consists of a multipass 16 L borosilicate glass cylinder reaction cell, homogeneously surrounded by 4 symmetrically arranged UV fluorescent lamps (Philips TL-K 40 W, $\lambda_{\text{max}} = 365$ nm) used to photochemically initiate the reaction. This chamber is coupled to a Nexus Thermo Nicolet FTIR spectrometer equipped with a liquid nitrogen cooled mercury cadmium telluride (MCT) detector for online infrared spectroscopy. The total path length of 96 m is obtained by using silver coated mirrors. The spectra were obtained by coadding 64 scans recorded at 2 cm⁻¹ instrumental resolution in the 650–4000 cm⁻¹ range. The second environmental chamber is equipped with GC–MS detection and consists in a 200 L Teflon bag surrounded by 8 UV lamps (Philips TL-K 40 W). Gas samples were analyzed by GC (Thermo Electron Co., model Trace GC Ultra) coupled to a mass spectrometer (Thermo Electron Co., model DSQ II).

Chlorine atoms were produced by the broad-band UV photolysis of Cl₂ in the bath gas (synthetic air). UV radiation was produced by the series of lamps symmetrically arranged around the outside of the FTIR cell and the Teflon bag. Reactants and Cl precursor were introduced directly into the chambers by expansion from a glass manifold system and mixed in synthetic air at 298 ± 2 K and 720 ± 2 Torr of total pressure.

Two reference compounds were used during our kinetic measurements: propene in the FTIR measurements and 1,3-butadiene in the GC–MS measurements. Concentrations in the reaction chambers for 3H3M2B and the reference compounds ranged from 10 to 15 ppm, whereas the concentrations of the precursors of Cl atoms (Cl₂) ranged from 15 to 25 ppm. Reactants were left to homogenize in the chamber for 60 min prior to irradiation. The kinetics of degradation of both the reference and the analyte inside the chamber was followed by monitoring the evolution of the areas of the absorption bands (by FTIR) by using the “abstraction” method based on calibrated reference spectra. In the GC–MS method, the degradation of 3H3M2B and the reference compound was monitored by following the decrease of the chromatographic peaks of both compounds as explained in the Results section. Samples were analyzed in situ into the pyrex cell by FTIR whereas in the Teflon bag, the concentrations were monitored by using the technique of solid-phase microextraction (SPME). SPME is a simple and effective adsorption and desorption technique, which eliminates the need of using solvents or complicated apparatus for concentrating volatile or nonvolatile compounds in liquid samples or headspaces.^{32,33} In this work, a 50/30 μ m divinylbenzene/carboxen/polydimethylsiloxane fiber was used. The coated fiber was inserted into the Teflon chamber and exposed during an optimized time of 15 min to the chamber contents. Then, SPME fiber samples were thermally desorbed in the heated (250 °C) GC injection port and the products were analyzed by mass spectrometry, thus the irradiation time was not continuous for the GC–MS system and the analysis was performed when the lamps were off.

Prior to analyses by using both techniques, a calibration of the measured concentration of the analyte and the detected products commercially available was carried out.

In addition to the standard constraint that consists of having a well-documented kinetic rate coefficient, the reference compound was chosen in such a way that its FTIR spectrum and/or chromatographic peak do not interfere with those of 3H3M2B and vice versa, and with the products of the reaction. The rate coefficient used in this work for the reaction of Cl with

propene was that reported by Ceacero-Vega et al.,³⁴ $(2.23 \pm 0.31) \times 10^{-10} \text{ cm}^3 \text{ molecule}^{-1} \text{ s}^{-1}$. For the rate coefficient of Cl atoms with 1,3-butadiene, the value of $(4.2 \pm 0.4) \times 10^{-10} \text{ cm}^3 \text{ molecule}^{-1} \text{ s}^{-1}$ at 760 Torr of air and 298 K was used.³⁵

2.2. Nature and Quantification of the Reaction Products. The products formed in the reaction of Cl atoms with 3H3M2B were investigated using both simulation chambers. These studies were performed under the same experimental conditions as those for the kinetic studies, but in the absence of reference compounds.

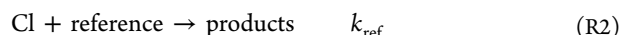
Samples were analyzed in situ by FTIR into the pyrex cell. The identification of the products was made by comparison with a library of IR spectra and with the IR spectrum of a pure sample. In the Teflon bag, the identification of the products was made by analysis of the mass spectrum by comparison with a library of spectra and the retention time and mass spectrum of a pure sample of the detected product. Under the conditions used here the SPME/GC–MS response was linear with the analyte concentration. No carryover was observed for any of the compounds upon a second injection, indicating a complete recovery of the fiber. The fiber was used immediately after desorption for the next sampling.

After each experiment, the reaction chamber was cleaned out by repeated purge-pump cycles until the reactants and/or products were not detected.

The purity of the used chemicals as stated by the manufacturer were 3H3M2B (95%), propene (99%), 1,3-butadiene (99%), 2,3-butanedione (97%), and acetic acid (99%) from Sigma-Aldrich and synthetic air (99.99%) from Air liquide.

3. RESULTS

3.1. Relative Rate Coefficient Measurements. In the conducted relative kinetic experiments the following reactions take place:



where $k_{3\text{H3M2B}}$ is the rate coefficient of the reaction of 3H3M2B with Cl and k_{ref} is the known rate coefficient of the reference compounds with Cl. Prior to kinetic measurements, experiments were performed in the absence of Cl precursor under radiation to determine the loss rate of the reactants (analyte and reference compound) due to photolysis. These tests were performed under light intensities and radiation time similar to those employed during our kinetic experiments in both simulation chambers. Further tests were performed in the absence of radiation for the 3H3M2B/Cl₂/air mixture to check for dark reactions and wall losses. The global secondary losses were 6%, 3%, and 4% for 3H3M2B, propene, and 1,3-butadiene, respectively, mainly coming from wall losses.

The 3H3M2B and reference compound concentration time evolution was described using the following expression taking into account these secondary loss processes:

$$\ln \frac{[3\text{H3M2B}]_0}{[3\text{H3M2B}]_t} - k_w t = \frac{k_{3\text{H3M2B}}}{k_{\text{ref}}} \times \left[\ln \frac{[\text{ref}]_0}{[\text{ref}]_t} - k'_w t \right] \quad (\text{I})$$

where $[3\text{H3M2B}]_0$, $[3\text{H3M2B}]_t$, $[\text{ref}]_0$, and $[\text{ref}]_t$ are the concentrations of the reagents before irradiation and at time t , respectively and k_w and k'_w are the decay rates resulting from

secondary losses for 3H3M2B and the reference compound, respectively. Figure 1 shows an example of this plot. A good

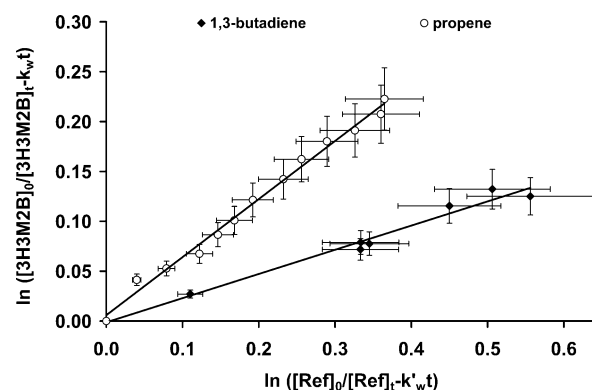


Figure 1. Examples of relative rate plots for the reaction of Cl with 3H3M2B with propene and 1,3-butadiene as reference compounds, according to eq I.

linearity is observed with a correlation coefficient greater than 99% and an intercept close to zero. The obtained rate coefficients are summarized in Table 1. For each point in Figure 1, the error bars indicate the total uncertainties on the experimental conditions as explained in the Discussion section.

Table 1. Rate Coefficient Ratios and the Obtained Relative Rate Coefficients for the Reaction of Cl Atoms with 3H3M2B at 298 ± 2 K and 720 ± 2 Torr

ref compd	detection technique	$k_{3\text{H3M2B}}/k_{\text{ref}}$	$k_{3\text{H3M2B}}$ ($10^{-10} \text{ cm}^3 \text{ molecule}^{-1} \text{ s}^{-1}$)
propene ^a	FTIR	0.53 ± 0.10	1.10 ± 0.30^c
		0.58 ± 0.06	1.30 ± 0.20^c
		0.49 ± 0.06	1.09 ± 0.20^c
		0.49 ± 0.05	1.10 ± 0.20^c
1,3-butadiene ^b	GC–MS	0.25 ± 0.04	1.06 ± 0.20^c
average			1.13 ± 0.17^d

^a $k(\text{propene}+\text{Cl}) = (2.23 \pm 0.31) \times 10^{-10} \text{ cm}^3 \text{ molecule}^{-1} \text{ s}^{-1}$ (Ceacero-Vega et al.³⁴). ^b $k(1,3\text{-butadiene}+\text{Cl}) = (4.2 \pm 0.4) \times 10^{-10} \text{ cm}^3 \text{ molecule}^{-1} \text{ s}^{-1}$ (Ragains and Finlayson-Pitts.³⁵). ^cUncertainty calculated according to eq II (see text). ^dTwice standard deviations.

As mentioned before, the kinetics of degradation of both the reference and the analyte inside the IR cell was followed by monitoring the evolution of the IR absorption bands areas of both compounds. The IR spectral features used for analysis were 1211–1149 cm^{-1} for 3H3M2B and 1005–971 cm^{-1} for propene.

In the Teflon bag chamber coupled to a GC–MS, the measurements were performed by following the evolution of the chromatographic peak areas of 3H3M2B and 1,3-butadiene with time at retention times of 4.75 and 1.95 min, respectively. The blank was analyzed before and after each sample analysis so as to minimize any uncertainties originating from the deviation of the MS signal and GC response.

3.2. Reaction Products and Mechanism. Products of the studied reaction were identified and quantified in the FTIR cell by using the FTIR spectroscopy and in the Teflon bag coupled to GC–MS.

The major primary oxidation products observed in the experiment carried out by FTIR were acetic acid, and CO. The

concentration–time profiles of 3H3M2B and acetic acid were obtained from integration of the IR spectra 1211–1149 cm^{-1} for 3H3M2B and 1890–1740 cm^{-1} for acetic acid. 2,3-Butanedione and formaldehyde were observed as well in FTIR analyses but were not quantified due to interferences with absorption peaks of other molecules occurring in the chemical mechanism of the studied reaction. 2,3-Butanedione was quantified by GC–MS as a major primary product. In addition to the above products, GC–MS analysis indicated the presence of chlorinated secondary reactions products and a number of small peaks that could not be identified. 2,3-Butanedione and secondary products were identified by comparison of their mass spectrum with the corresponding spectra from a spectral library and also the mass spectrum and retention time of a commercial sample. Figures 2 and 3 show an example of an IR spectra and a

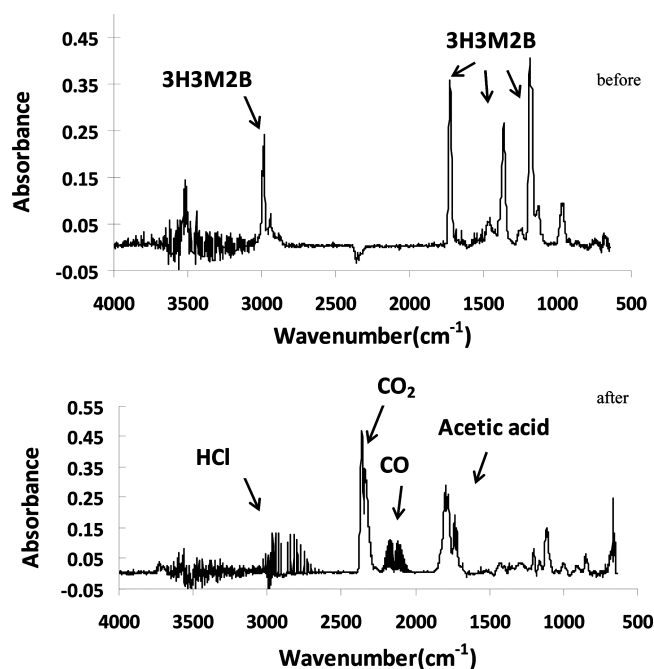


Figure 2. Example of infrared absorption spectra recorded in this work. The upper trace shows the infrared spectrum of the Cl_2 /3H3M2B mixture in 720 Torr of synthetic air in the FTIR cell before irradiation, and the lower trace shows the spectrum 60 min after the start of irradiation.

gas chromatogram taken before irradiation and 60 min after irradiation of a 3H3M2B/ Cl_2 /air mixture in the FTIR cell and the Teflon bag, respectively. The temporal evolution of 3H3M2B and main reaction products is shown in Figures 4 and 5. The concentration profiles of acetic acid and 2,3-butanedione show that both are primary products. The formation yields of the major products detected in this study represent the slopes of the plot of $[\text{product}]_t/[\text{3H3M2B}]_0$ vs $1 - [\text{3H3M2B}]_t/[\text{3H3M2B}]_0$, where $[\text{product}]_t$ is the product concentration at a time t and $[\text{3H3M2B}]_0$ and $[\text{3H3M2B}]_t$ are the 3H3M2B concentrations before irradiation and at time t , respectively (Figures 6 and 7). The formation yields of the products can be derived from the slopes of these plots, and the obtained values were $42.6 \pm 4.8\%$ and $17.2 \pm 2.3\%$ for acetic acid and 2,3-butanedione, respectively. The carbon balance obtained was 33.1%, showing that additional formed oxidation products could not be detected or quantified.

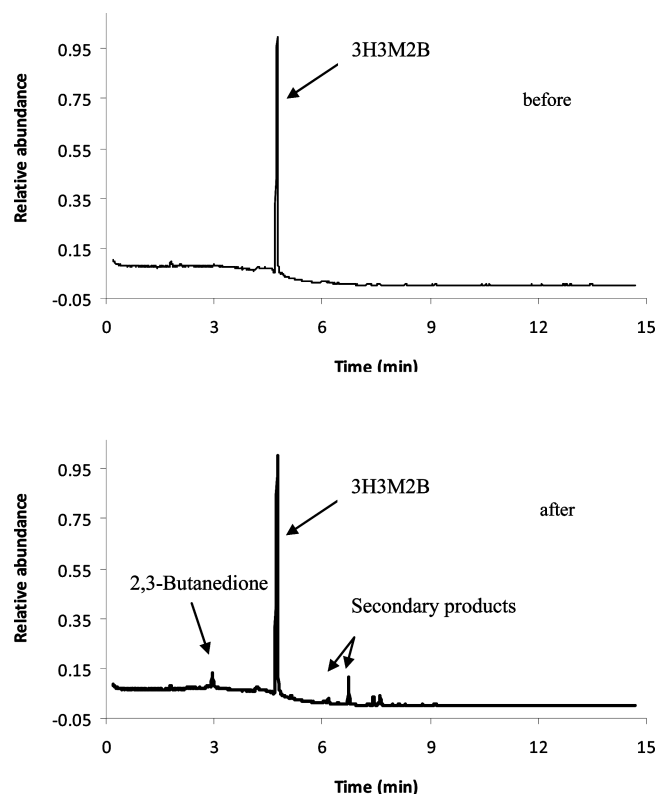


Figure 3. Gas chromatograms of samples from a Cl_2 /3H3M2B mixture in 720 Torr of synthetic air in the Teflon bag before and 60 min after the start of irradiation.

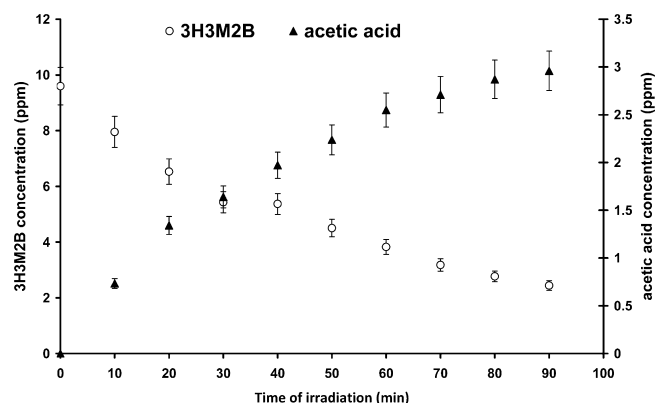


Figure 4. Plot of the concentration of 3H3M2B and acetic acid versus the time of reaction. Analyses were carried out by FTIR.

4. DISCUSSION

4.1. Error Analysis. The overall error in the rate coefficient values reported in this work (Table 1) varies from 17 to 26%. This error originates from the uncertainty on the rate coefficient of the reference compounds used in this study and the errors on the determination of the slope k/k_{ref} shown in Figure 1. The error on the rate coefficient is therefore calculated according to eq II:

$$\Delta k = k \times \sqrt{\left[\frac{\Delta k_{\text{ref}}}{k_{\text{ref}}}\right]^2 + \left[\frac{\Delta(\text{slope})}{\text{slope}}\right]^2} \quad (\text{II})$$

The errors on k_{ref} as found in the literature were 13.9 and 9.5% for propene and 1,3-butadiene, respectively.

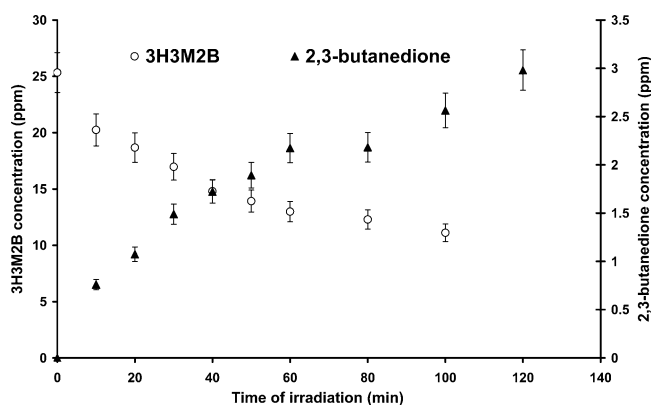


Figure 5. Plot of the concentration of 3H3M2B and 2,3-butanedione versus the time of reaction. Analyses were carried out by SPME/GC–MS.

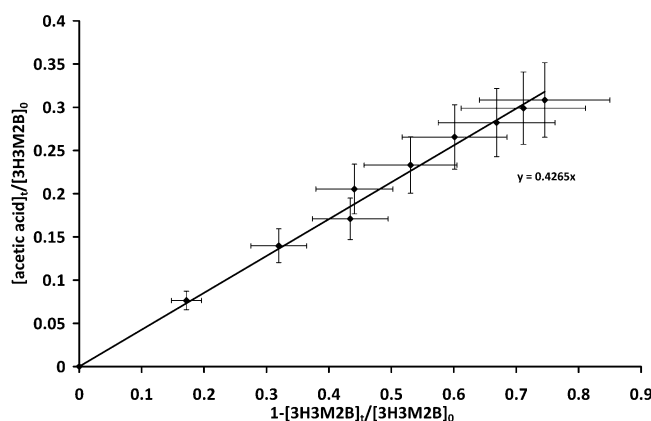


Figure 6. Plot of the ratio of acetic acid formed over the initial concentration of 3H3M2B versus reacted 3H3M2B.

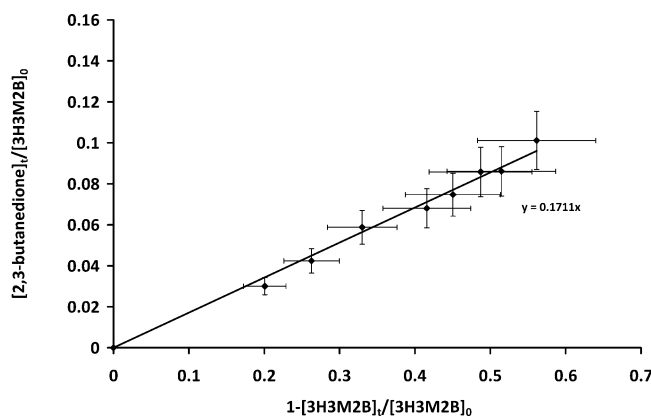


Figure 7. Plot of the ratio of 2,3-butanedione formed over the initial concentration of 3H3M2B versus reacted 3H3M2B.

The errors on the slope originate from

- statistical errors that result from a least-squares analysis of Figure 1, multiplied by the Student's *t*-factor appropriate for the 95% confidence interval and the number of degrees of freedom and
- systematic errors that are estimated to 7%.

The systematic errors originate from the difficulties in measuring the concentrations of the studied reagents with good accuracy due to the temperature instability, the difficulties in

handling 3H3M2B because of its low vapor pressure, and the purity degree of the used compounds. To minimize these uncertainties, several preliminary tests were carried out such as the GC column temperature and the selection of the reference compound to have relatively intense chromatograms and spectroscopic peaks.

Individual vertical and horizontal error bars on each point in Figure 1 correspond to 14%. The error reported on the average rate coefficient given in Table 1 is two standard deviations.

In addition to the systematic errors cited above, the error in the formation yield values reported in this work originate from statistical errors that result from a least-squares analysis of the $[\text{product}]_t/[\text{3H3M2B}]_0$ vs $1 - [\text{3H3M2B}]_t/[\text{3H3M2B}]_0$ plot, multiplied by the Student's *t*-factor appropriate for the 95% confidence interval and the number of degrees of freedom. The overall error on the formation yield obtained in this work was about 11% and 13% for acetic acid and 2,3-butanedione, respectively.

4.2. Comparison with the Literature and the Effect of the Structure on the Reactivity.

This work provides the first kinetic study of the gas-phase reaction of 3H3M2B with Cl atoms. As mentioned before, the degradation of 3H3M2B by OH, NO₃, and O₃ has been investigated by Aschmann et al.¹⁴ The measured rate coefficient for the reaction of 3H3M2B with Cl atoms obtained in this work, $(1.13 \pm 0.17) \times 10^{-10} \text{ cm}^3 \text{ molecule}^{-1} \text{ s}^{-1}$, is about 120 times that reported in the literature for the reaction with OH, $(0.94 \pm 0.08) \times 10^{-12} \text{ cm}^3 \text{ molecule}^{-1} \text{ s}^{-1}$.

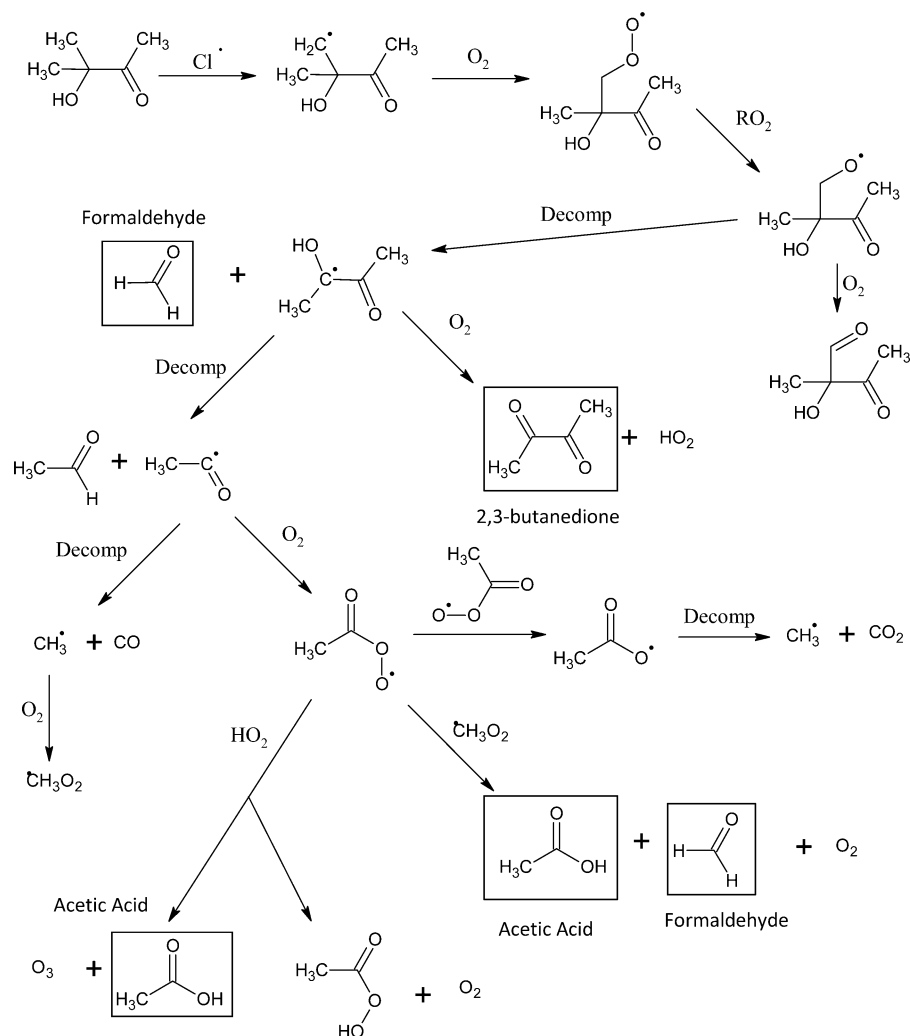
The calculated value for the reaction of Cl atoms with 3H3M2B by the SAR method is $5.7 \times 10^{-11} \text{ cm}^3 \text{ molecule}^{-1} \text{ s}^{-1}$,³⁶ using a factor $F(\text{CO}) = 0.12$ derived from the experimental value for the reaction of Cl atoms with butanone of $(4.08 \pm 0.21) \times 10^{-11} \text{ cm}^3 \text{ molecule}^{-1} \text{ s}^{-1}$.³⁷ This calculated value is about 50% lower than the present measurement. This discrepancy is due to the fact that activating effects are not considered in this calculation.

The comparison of the rate coefficient for 3H3M2B obtained in this work to that of 3-methyl-2-butanone ($\text{CH}_3)_2\text{CHC}(\text{O})\text{CH}_3$ ($6.2 \pm 0.5) \times 10^{-11} \text{ cm}^3 \text{ molecule}^{-1} \text{ s}^{-1}$ reported by Kaiser and Wallington³⁸ suggests that the reaction with Cl proceeds mainly via H-abstraction of the weakest C–H bond on the two $-\text{CH}_3$ groups activated by the presence of the $-\text{OH}$ substituent group. The same behavior has been observed for reactions of 2-butanone, 3H2B, and 4H2B with Cl atoms.^{16,37,39}

Our value is compared to that of reaction of Cl with 3-hydroxy-2-butanone (3H2B) where the OH group is in the α position with respect to the carbonyl group similarly to 3H3M2B. The rate coefficient for the gas-phase reactions of Cl atoms with 3-hydroxy-2-butanone was measured by Messaadia et al.¹⁶ using an atmospheric simulation chamber made of Teflon at 298 \pm 3 K and 760 Torr. The obtained rate coefficient was $(4.90 \pm 0.45) \times 10^{-11} \text{ cm}^3 \text{ molecule}^{-1} \text{ s}^{-1}$. This comparison shows that the reactivity of these species with Cl increases by a factor of 2.3 when an H atom attached to the carbon atom α to the $>\text{C}=\text{O}$ group is replaced by a methyl group. As for other ketones,^{39–41} the $>\text{C}=\text{O}$ group seems to deactivate the C–H bonds attached to carbon atom α to the $>\text{C}=\text{O}$ group for hydroxyketones and to activate the C–H bonds attached to carbon atom β to the $>\text{C}=\text{O}$ group as for 4H2B.

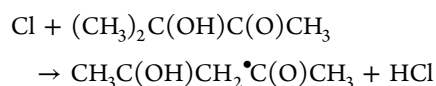
4.3. Mechanism. As seen in Figures 6 and 7, a good linearity is observed for the plot of $[\text{product}]_t/[\text{3H3M2B}]_0$ vs 1

Scheme 1. Proposed Mechanism for the Reaction of Cl Atoms with 3H3M2B, Where Detected Products Are Shown in a Box



– $[\text{3H3M2B}]_t/[\text{3H3M2B}]_0$ with a correlation coefficient higher than 99% showing that acetic acid and 2,3-butanedione are the major primary oxidation products of the studied reaction. This result suggests that the reaction of 3H3M2B with Cl may proceed mainly via H-abstraction of the weakest C–H bond on the two $-\text{CH}_3$ groups in the β position with respect to the carbonyl group. In Scheme 1 is shown the mechanism of the oxidation of 3H3M2B by the chlorine atoms. This scheme includes different reaction pathways that may occur and may explain the formation of different products which have been identified in this work.

Initially, the abstraction mainly proceeds through the following channel:



The primary radical formed $\text{CH}_3\text{C}(\text{OH})\text{CH}_2^\bullet\text{C}(\text{O})\text{CH}_3$ will react with O_2 followed by reaction with RO_2 to lead to the corresponding radical $\text{CH}_3\text{C}(\text{OH})\text{CH}_2\text{O}^\bullet\text{C}(\text{O})\text{CH}_3$. This radical may react with O_2 or decompose. Decomposition may lead to the $\text{CH}_3\text{C}^\bullet(\text{OH})\text{C}(\text{O})\text{CH}_3$ radical and to formaldehyde HCHO , which was detected by FTIR but not quantified due to interferences with absorption peaks of other molecules occurring in the chemical mechanism of the studied reaction.

The $\text{CH}_3\text{C}^\bullet(\text{OH})\text{C}(\text{O})\text{CH}_3$ radical may react with O_2 to form 2,3-butanedione $\text{CH}_3\text{C}(\text{O})\text{C}(\text{O})\text{CH}_3$ identified and quantified by GC–MS analysis.

In addition to 2,3-butanedione, acetic acid CH_3COOH was observed in this work as a major product. We suggest here a mechanism that could explain the formation of acetic acid as a primary product of the reaction of 3H3M2B with Cl.

The $\text{CH}_3\text{C}^\bullet(\text{OH})\text{COCH}_3$ radical formed after the decomposition of the $\text{CH}_3\text{C}(\text{OH})\text{CH}_2\text{O}^\bullet\text{C}(\text{O})\text{CH}_3$ radical may decompose to lead to the formation of the $\text{CH}_3\text{C}^\bullet(\text{O})$ radical and ethanal CH_3CHO . The $\text{CH}_3\text{C}^\bullet(\text{O})$ radical may decompose to lead to the formation of CO (observed at the beginning of the reaction) and the CH_3 radical, which may generate the methylperoxy radical CH_3O_2 after reaction with O_2 . The $\text{CH}_3\text{C}^\bullet(\text{O})$ radical may also react with O_2 to yield the $\text{CH}_3\text{C}(\text{O})\text{OO}^\bullet$ radical. This radical may react through three possible pathways: It might react with itself to give the $\text{CH}_3\text{C}(\text{O})\text{O}^\bullet$ radical, which decomposes to generate the CH_3 radical and CO_2 .⁴² Another possible path leading to the production of the observed acetic acid can result from the reaction of the $\text{CH}_3\text{C}(\text{O})\text{OO}^\bullet$ radical with HO_2 . The yield of acetic acid for this reaction is $20 \pm 8\%$, as reported by Orlando and Tyndall.⁴³ The radical–radical reaction of $\text{CH}_3\text{C}(\text{O})\text{OO}^\bullet$ with $^\bullet\text{CH}_3\text{O}_2$ has been previously studied^{42,44–46} and shown to proceed through two main channels: the first one (a) leads to

the formation of $\text{CH}_3\text{C}(\text{O})\text{O}^\bullet$, CH_3O , and O_2 and the second one (b) leads to the formation of acetic acid, formaldehyde and O_2 . Different values of the branching ratios of channel (a) have been reported in the literature, varying from 0.48 to 0.90.⁴² Therefore, the yield of acetic acid for this reaction should be in the range 10–52%.

5. TROPOSPHERIC IMPLICATIONS

It is known that volatile organic compounds, in general, are chemically removed from the troposphere mainly by reaction with the tropospheric oxidants: OH, NO_3 , O_3 , and halogen atoms. The tropospheric lifetime (τ) of any volatile organic compound due to its reaction with an oxidant X is commonly defined by

$$\tau = \frac{1}{k_x[\text{X}]} \quad (\text{III})$$

where k_x is the rate coefficient of the organic compound with the X oxidant which is present in the troposphere in an average concentration [X].

A tropospheric lifetime for the reaction of Cl atoms with 3H3M2B of 102 days was calculated according to eq III where [Cl] represents the 24 h daytime average global tropospheric concentration of Cl atoms of 1×10^3 molecules cm^{-3} .⁴⁷ Therefore, despite their high reactivity, Cl atoms concentrations are too low to compete with OH radicals in influencing the oxidizing capacity of the global troposphere. The reactions with Cl atoms, however, could be an important loss process for these species in coastal areas where the concentration of Cl atoms reaches 1×10^5 molecules cm^{-3} ,²⁴ and the tropospheric lifetime is therefore reduced to about 1 day. The lifetimes due to the reactions with OH, NO_3 , and O_3 as reported by Aschmann et al.¹⁴ were (in days) 12, >230, and >150, respectively. These values were calculated by using a 24 h average concentration of 1×10^6 molecules cm^{-3} for OH, 2.5×10^8 molecules cm^{-3} for NO_3 , and 7×10^{11} molecules cm^{-3} for O_3 .

Until now, there has been no study concerning the wet and dry deposition of 3H3M2B. However, the photolysis of a series of hydroxyketones including 3H3M2B has been studied by Messaadia et al.¹⁸ An upper limit of photodissociation rate coefficient (J_p) for the studied compound of 0.4 day corresponding to a zenith angle of 30° and between 200 and 345 nm was calculated by these authors considering a quantum yield of unity. It should be noted that the overall quantum yield in the actinic region for 3H3M2B is not known. However, the quantum yield for smaller hydroxyketones such as hydroxyacetone has been measured by Orlando et al.¹² who obtained an upper value of 0.6 for wavelengths greater than 290 nm. In the present work, a lifetime of 3H3M2B due to photolysis of 0.76 day is calculated by using the upper limit of quantum yield of hydroxyacetone (Table 2).

Reactions with Cl in marine areas and photolysis seem to be the main loss processes for 3H3M2B provided that the assumption with respect to the quantum yield is correct.

In the light of the products detected in this work, the reactions of 3H3M2B with Cl may contribute to the photochemical pollution in contaminated coastal urban areas. In addition, the developed mechanism to explain the products observations via FTIR or GC–MS in the present work suggests the formation of $\text{CH}_3\text{C}(\text{O})\text{OO}^\bullet$ radical (Scheme 1). Therefore, it is important to stress that the atmospheric degradation of

Table 2. Tropospheric Lifetimes (days) of 3H3M2B Due to Photolysis and Its Gas-Phase Reactions with Atmospheric Photooxidants

$\tau_{\text{photolysis}}^a$	τ_{OH}^b	$\tau_{\text{NO}_3}^b$	$\tau_{\text{O}_3}^b$	τ_{Cl}^c
>0.76	12	>230	>150	102

^aCalculated using the photolysis rate for hydroxyacetone determined by Orlando et al.¹² and the absorption cross sections determined by Messaadia et al.¹⁸ (see text). ^bCalculated by Aschmann et al.,¹⁴ with a OH 24 h average concentration of 1×10^6 molecules cm^{-3} , a 24 h average NO_3 concentration of 2.5×10^8 molecules cm^{-3} , and a 24 h average O_3 concentration of 7×10^{11} molecules cm^{-3} . ^cCalculated by using the rate constant determined in this work with an upper limit of 1×10^3 molecules cm^{-3} reported by Wingenter et al.⁴¹

3H3M2B in the presence of NO_x can be a source of other toxic molecules with high atmospheric interest such as PAN which could be formed from the reaction of $\text{CH}_3\text{C}(\text{O})\text{OO}^\bullet$ with NO_2 .

6. CONCLUSION

This work constitutes the first kinetic and mechanistic studies of the reaction of Cl with 3H3M2B. The kinetic measurements were investigated using a relative method at room temperature and at atmospheric pressure. The obtained data showed that the reaction of the studied compound with Cl atoms proceeds more rapidly than that with OH radicals. Our results are consistent with the expectation that the presence of the carbonyl group deactivates the C–H bonds attached to the carbon atom α to the $>\text{C}=\text{O}$ group and activates those attached to the carbon atom β to the $>\text{C}=\text{O}$ group.

The reaction of 3H3M2B with Cl is suggested to mainly proceed via H-abstraction of the weakest C–H bond on the two $-\text{CH}_3$ groups in the β position with respect to the carbonyl group. The major products quantified in this work were acetic acid and 2,3-butanedione.

The calculated tropospheric lifetime obtained in this work suggests that the reactions with Cl atoms could be an important loss process for these species in coastal areas and contributes to the photochemical pollution in these areas.

It is important to note that the above analysis does not take into account any heterogeneous loss processes for 3H3M2B. Moreover, there is a need to determine the photolysis quantum yields of the studied compound and to measure its photolysis rates under simulated atmospheric conditions.

AUTHOR INFORMATION

Corresponding Author

*G. El Dib. Tel.: +33 2 23 23 56 80. Fax: +33 2 23 23 67 86. E-mail address: gisele.eldib@univ-rennes1.fr.

Notes

The authors declare no competing financial interest.

ACKNOWLEDGMENTS

The authors gratefully thank the INSU-LEFE French programme, the Brittany Region and the doctoral school SDLM at the University of Rennes 1 for financial support. They would like to thank as well the Spanish Ministerio de Ciencia e Innovación (Project CGL2010-19066) for the financial support of this research work.

REFERENCES

- (1) de Andrade, M. V. A. S.; Pinheiro, H. L. C.; Pereira, P. A. D.; de Andrade, J. B. *Quim. Nova* **2002**, 25, 1117–1131.

- (2) Ciccioli, P.; Brancaleoni, E.; Frattoni, M.; Cecinato, A.; Brachetti, A. *Atmos. Environ.* **1993**, *27*, 1891–1901.
- (3) Baugh, J.; Ray, W.; Black, F.; Snow, R. *Atmos. Environ.* **1987**, *21*, 2077–2082.
- (4) Kesselmeier, J.; Staudt, M. *J. Atmos. Chemistry* **1999**, *33*, 23–88.
- (5) Schauer, J. J.; Kleeman, M. J.; Cass, G. R.; Simoneit, B. R. T. *Environ. Sci. Technol.* **2001**, *35*, 1716–1728.
- (6) Grosjean, D.; Williams, E. L.; Grosjean, E.; Andino, J. M.; Seinfeld, J. H. *Environ. Sci. Technol.* **1993**, *27*, 2754–2758.
- (7) Rivas, B.; Torre, P.; Dominguez, J. M.; Perego, P.; Converti, A.; Parajo, J. C. *Biotechnol. Prog.* **2003**, *19*, 706–713.
- (8) Ichikawa, N.; Sato, S.; Takahashi, R.; Sodesawa, T. *Catal. Commun.* **2005**, *6*, 19–22.
- (9) Dillon, T. J.; Horowitz, A.; Holscher, D.; Crowley, J. N.; Vereecken, L.; Peeters, J. *Phys. Chem. Chem. Phys.* **2006**, *8*, 236–246.
- (10) Butkovskaya, N. I.; Pouvesle, N.; Kukui, A.; Mu, Y. J.; Le Bras, G. *J. Phys. Chem. A* **2006**, *110*, 6833–6843.
- (11) Dagaut, P.; Liu, R. Z.; Wallington, T. J.; Kurylo, M. J. *J. Phys. Chem. A* **1989**, *93*, 7838–7840.
- (12) Orlando, J. J.; Tyndall, G. S.; Fracheboud, J. M.; Estupinan, E. G.; Haberkorn, S.; Zimmer, A. *Atmos. Environ.* **1999**, *33*, 1621–1629.
- (13) Stoeffler, C.; Joly, L.; Durry, G.; Cousin, J.; Dumelie, N.; Bruyant, A.; Roth, E.; Chakir, A. *Chem. Phys. Lett.* **2013**, *590*, 221–226.
- (14) Aschmann, S. M.; Arey, J.; Atkinson, R. *J. Phys. Chem. A* **2000**, *104*, 3998–4003.
- (15) Baker, J.; Arey, J.; Atkinson, R. *J. Phys. Chem. A* **2004**, *108*, 7032–7037.
- (16) Messaadia, L.; El Dib, G.; Lendar, M.; Cazaunau, M.; Roth, E.; Ferhati, A.; Mellouki, A.; Chakir, A. *Atmos. Environ.* **2013**, *77*, 951–958.
- (17) El Dib, G.; Sleiman, C.; Canosa, A.; Travers, D.; Courbe, J.; Sawaya, T.; Mokbel, I.; Chakir, A. *J. Phys. Chem. A* **2013**, *117*, 117–125.
- (18) Messaadia, L.; El Dib, G.; Ferhati, A.; Roth, E.; Chakir, A. *Chem. Phys. Lett.* **2012**, *529*, 16–22.
- (19) Thornton, J. A. *Nature* **2010**, *464*, 271–274.
- (20) Cavender, A. E.; Biesenthal, T. A.; Bottenheim, J. W.; Shepson, P. B. *Atmos. Chem. Phys.* **2008**, *8*, 1737–1750.
- (21) Riedel, T. P.; Wagner, N. L.; Dube, W. P.; Middle, A. N.; Young, C. J.; Öztürk, F.; Bahreini, R.; VandenBoer, T. C.; Wolfe, D. E.; Williams, E. J.; Roberts, J. M.; Brown, S. S.; Thornton, J. A. *J. Geophys. Res. Atmos.* **2013**, *118*, 8702–8715.
- (22) Jobson, B. T.; Niki, H.; Yokouchi, Y.; Bottenheim, J.; Hopper, F.; Leaitch, R. *J. Geophys. Res.-Atmos.* **1994**, *99*, 25355–25368.
- (23) Keil, A. D.; Shepson, P. B. *J. Geophys. Res.-Atmos.* **2006**, *111*, DOI: 10.1029/2006JD007119.
- (24) Singh, H. B.; Thakur, A. N.; Chen, Y. E.; Kanakidou, M. *Geophys. Res. Lett.* **1996**, *23*, 1529–1532.
- (25) Spicer, C. W.; Chapman, E. G.; Finlayson-Pitts, B. J.; Plastridge, R. A.; Hubbe, J. M.; Fast, J. D.; Berkowitz, C. M. *Nature* **1998**, *394*, 353–356.
- (26) Hein, R.; Crutzen, P. J.; Heimann, M. *Global Biogeochemical Cycles* **1997**, *11*, 43–76.
- (27) Lawrence, M. G.; Jockel, P.; von Kuhlmann, R. *Atmos. Chem. Phys.* **2001**, *1*, 37–49.
- (28) Atkinson, R.; Baulch, D. L.; Cox, R. A.; Hampson, R. F.; Kerr, J. A.; Troe, J. *J. Phys. Chem. Ref. Data* **1989**, *18*, 881–1097.
- (29) Ballesteros, B.; Ceacero-Vega, A. A.; Garzon, A.; Jimenez, E.; Albaladejo, J. *J. Photochem. Photobiol. A-Chem.* **2009**, *208*, 186–194.
- (30) Ceacero-Vega, A. A.; Ballesteros, B.; Bejan, I.; Barnes, I.; Albaladejo, J. *ChemPhysChem* **2011**, *12*, 2145–2154.
- (31) Ceacero-Vega, A. A.; Ballesteros, B.; Bejan, I.; Barnes, I.; Jimenez, E.; Albaladejo, J. *J. Phys. Chem. A* **2012**, *116*, 4097–4107.
- (32) Alpendurada, M. D. *J. Chromatogr. A* **2000**, *889*, 3–14.
- (33) Arthur, C. L.; Pawliszyn, J. *Anal. Chem.* **1990**, *62*, 2145–2148.
- (34) Ceacero-Vega, A. A.; Ballesteros, B.; Albaladejo, J.; Bejan, I.; Barnes, I. *Chem. Phys. Lett.* **2009**, *484*, 10–13.
- (35) Ragains, M. L.; FinlaysonPitts, B. J. *J. Phys. Chem. A* **1997**, *101*, 1509–1517.
- (36) Aschmann, S. M.; Atkinson, R. *Int. J. Chem. Kinet.* **1995**, *27*, 613–622.
- (37) Takahashi, K.; Iwasaki, E.; Matsumi, Y.; Wallington, T. J. *J. Phys. Chem. A* **2007**, *111*, 1271–1276.
- (38) Kaiser, E. W.; Wallington, T. J. *J. Phys. Chem. A* **2007**, *111*, 10667–10670.
- (39) Albaladejo, J.; Notario, A.; Cuevas, C. A.; Jimenez, E.; Cabanas, B.; Martinez, E. *Atmos. Environ.* **2003**, *37*, 455–463.
- (40) Iwasaki, E.; Taketani, F.; Takahashi, K.; Matsumi, Y.; Wallington, T. J.; Hurley, M. D. *Chem. Phys. Lett.* **2007**, *439*, 274–279.
- (41) Wallington, T. J.; Guschin, A.; Hurley, M. D. *Int. J. Chem. Kinet.* **1998**, *30*, 309–310.
- (42) Roehl, C. M.; Bauer, D.; Moortgat, G. K. *J. Phys. Chem.* **1996**, *100*, 4038–4047.
- (43) Orlando, J. J.; Tyndall, G. S. *Chem. Soc. Rev.* **2012**, *41*, 6294–6317.
- (44) Moortgat, G. K.; Veyret, B.; Lesclaux, R. *J. Phys. Chem.* **1989**, *93*, 2362.
- (45) Horie, O.; Moortgat, G. K. *J. Chem. Soc., Faraday Trans.* **1992**, *88*, 3305 and personal communication..
- (46) Lesclaux, R.; Boyd, A.; Noziere, B.; Villenave, E. LABVOC Report, Project EVSV-CT91-0038: Second Annual Report, Aug 4, 1994.
- (47) Wingenter, O. W.; Blake, D. R.; Blake, N. J.; Sive, B. C.; Rowland, F. S.; Atlas, E.; Flocke, F. *J. Geophys. Res.-Atmos.* **1999**, *104*, 21819–21828.